ARTICLE

doi:10.1038/nature10812

Piezo proteins are pore-forming subunits of mechanically activated channels

Bertrand Coste[1]*, Bailong Xiao[1]*, Jose S. Santos[2], Ruhma Syeda[2], Jörg Grandl[1]†, Kathryn S. Spencer[1], Sung Eun Kim[1], Manuela Schmidt[1], Jayanti Mathur[3], Adrienne E. Dubin[1], Mauricio Montal[2] & Ardem Patapoutian[1,3]

Mechanotransduction has an important role in physiology. Biological processes including sensing touch and sound waves require as-yet-unidentified cation channels that detect pressure. Mouse Piezo1 (MmPiezo1) and MmPiezo2 (also called Fam38a and Fam38b, respectively) induce mechanically activated cationic currents in cells; however, it is unknown whether Piezo proteins are pore-forming ion channels or modulate ion channels. Here we show that *Drosophila melanogaster* Piezo (DmPiezo, also called CG8486) also induces mechanically activated currents in cells, but through channels with remarkably distinct pore properties including sensitivity to the pore blocker ruthenium red and single channel conductances. MmPiezo1 assembles as a ~1.2-million-dalton homo-oligomer, with no evidence of other proteins in this complex. Purified MmPiezo1 reconstituted into asymmetric lipid bilayers and liposomes forms ruthenium-red-sensitive ion channels. These data demonstrate that Piezo proteins are an evolutionarily conserved ion channel family involved in mechanotransduction.

Mechanically activated currents have been described in various mammalian cells, including inner ear hair cells[1], somatosensory dorsal root ganglion neurons[2], vascular smooth muscle cells[3] and kidney primary epithelia[4]. Most of these mechanically activated currents are cationic with Ca^{2+} permeability, leading to a search for cation channels able to convert mechanical forces into such currents. Few mechanically activated channels have been described so far[5–7]; however, none of the candidates has been shown convincingly to mediate the physiologically relevant non-selective cationic mechanically activated currents in mammals.

MmPiezo1 was recently identified as a protein required for mechanically activated currents in a mammalian cell line. Expressing MmPiezo1 or related MmPiezo2 in a variety of mammalian cell lines induces mechanically activated cationic currents[8]. MmPiezo1-induced currents are inhibited by GsMTx4 (*Grammostola spatulata* mechanotoxin 4), a peptide widely used to study mechanically activated channels[9]. MmPiezo1 and MmPiezo2 contain over 30 putative transmembrane domains and do not resemble known ion channels or other protein classes. Piezo proteins could be non-conducting subunits of cationic ion channels required for proper expression or for modulating channel properties[6,10,11]. Alternatively, Piezo proteins may define a novel class of ion channels involved in mechanotransduction.

Mechanosensitivity of DmPiezo

Piezo sequences are present in the genomes of many animal, plant and other eukaryotic species. Functional analysis of Piezo proteins from phylogenetically distant species could demonstrate a conserved role of these proteins in mechanotransduction; furthermore, a comparative analysis of mechanically activated currents could elucidate unique pore properties of channels induced by Piezo proteins from distinct species. We focused on the apparently single member of *D. melanogaster* Piezo (DmPiezo), as this invertebrate species is widely used to study mechanotransduction using genetic approaches[12–16]. DmPiezo is 24% identical to mammalian Piezo proteins, with sequence conservation throughout the length of the proteins (Supplementary Fig. 1). We cloned the full-length DmPiezo complementary DNA into pIRES2-EGFP vector. We recorded mechanically activated currents from fluorescent HEK293T cells expressing DmPiezo-pIRES2-EGFP by applying force to the cell surface while monitoring transmembrane currents at constant voltage using patch-clamp recordings in the whole-cell configuration[2,17,18]. DmPiezo, but not mock-transfected cells, showed large mechanically activated currents (Fig. 1a, b). These currents have a time constant of inactivation τ of 6.2 ± 0.3 ms ($n = 32$ cells) at -80 mV when fitted with mono-exponential function, which is faster than observed for MmPiezo1 (~16 ms) and more comparable to MmPiezo2 (~7 ms)[8]. Similar to its mammalian counterparts, DmPiezo mechanically activated currents are characterized by a linear current–voltage (I–V) relationship with a reversal potential around 0 mV, consistent with it mediating a non-selective cationic conductance (Fig. 1c). We further characterized DmPiezo-induced currents in HEK293T cells in response to negative pressure pulses applied through the recording pipette in the cell-attached mode, an alternative mechanosensitivity assay. Overexpression of DmPiezo induced stretch-activated currents (Fig. 1d, e) with a pressure for half-maximal activation (P_{50}) of -31.8 ± 2.8 mm Hg (Fig. 1f), similar to the P_{50} calculated for MmPiezo1-induced currents (~30 mm Hg)[8]. Therefore, mechanosensitivity of the Piezo family is conserved in invertebrates. We demonstrate the physiological relevance of DmPiezo *in vivo* in an accompanying paper[19].

Pore properties of Piezo proteins

We next compared fundamental permeation properties of MmPiezo1 and DmPiezo. Ruthenium red, a polycationic pore blocker of TRP channels[20,21], blocks MmPiezo1- and MmPiezo2-induced mechanically activated currents[8]. We found that ruthenium red is a voltage-dependent blocker of MmPiezo1, with an IC_{50} value of 5.4 ± 0.9 μM at -80 mV (Fig. 2a–c): at a concentration of 30 μM, extracellular ruthenium red inhibited inward mechanically activated currents without affecting

[1]Department of Cell Biology, Dorris Neuroscience Center, The Scripps Research Institute, La Jolla, California 92037, USA. [2]Section of Neurobiology, Division of Biological Sciences, University of California San Diego, La Jolla, California 92093, USA. [3]Genomic Institute of the Novartis Research Foundation, San Diego, California 92121, USA. †Present address: Department of Neurobiology, Duke University Medical Center, Durham, North Carolina 27710, USA.
*These authors contributed equally to this work.

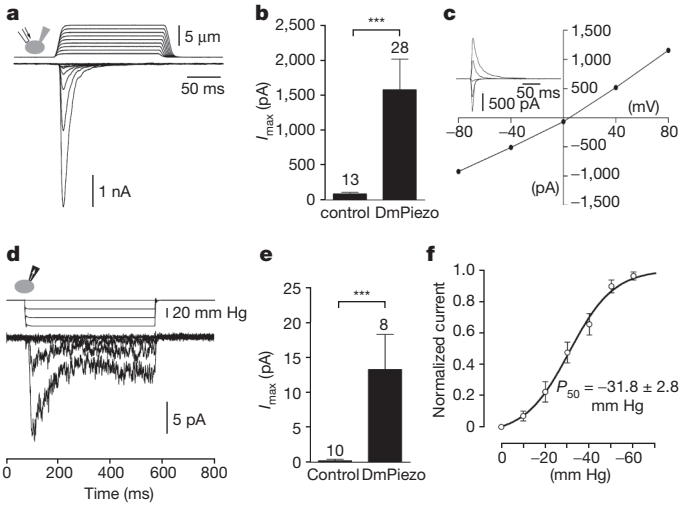

Figure 1 | Human cells expressing *Drosophila* Piezo (DmPiezo) show large mechanically activated currents. **a**–**f**, Mechanically activated currents of DmPiezo-expressing HE293T cells recorded in the whole-cell (**a**–**c**) or cell-attached (**d**–**f**) configuration. **a**, Representative traces of mechanically activated inward currents at −80 mV in DmPiezo-transfected cells subjected to a series of mechanical steps in 1 µm increments. **b**, Average maximal current amplitude of mechanically activated inward currents at −80 mV. **c**, Representative *I*–*V* relationship of mechanically activated currents in DmPiezo-transfected cells. The inset shows mechanically activated currents evoked at holding potentials ranging from −80 to +80 mV. **d**, Representative currents elicited by negative pipette pressure (0 to −60 mm Hg, Δ20 mm Hg) in DmPiezo-transfected cells. **e**, Average maximal current amplitude of stretch-activated currents at −80 mV. **f**, I_{max} normalized current–pressure relationship of stretch-activated currents recorded at −80 mV in DmPiezo-transfected cells ($n = 8$ cells) and fitted with a Boltzmann equation. P_{50} is the average of P_{50} values determined for individual cells. Bars represent mean ± s.e.m. and the number of cells tested is shown above bars. ***$P < 0.001$, Mann–Whitney *U*-test.

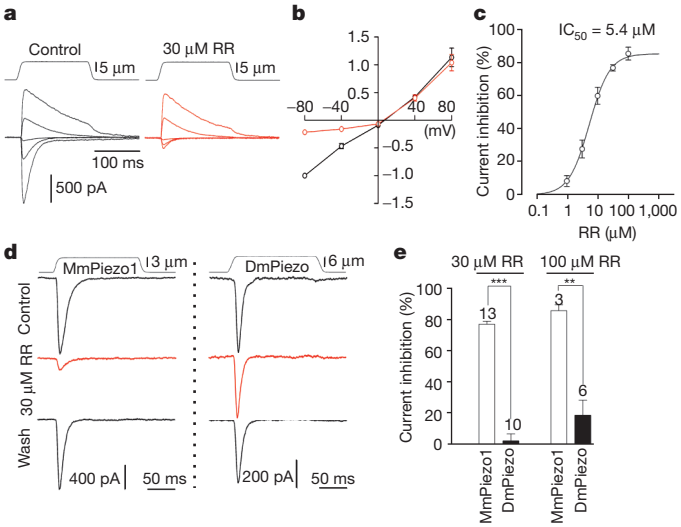

Figure 2 | Ruthenium red is a channel pore blocker of MmPiezo1- but not DmPiezo-induced currents. **a**, Representative traces of mechanically activated currents in MmPiezo1-transfected cells evoked at holding potentials ranging from −80 to +80 mV before (left panel) and during perfusion of 30 µM of ruthenium red (right panel, red traces). **b**, Average *I*–*V* relationship of mechanically activated currents in MmPiezo1-transfected cells ($n = 7$ cells) before (black symbols) and during (red symbols) perfusion of 30 µM ruthenium red. Currents were normalized to the value of control current evoked at −80 mV for each individual cell. **c**, Concentration-inhibition curve for ruthenium red (RR) on mechanically activated currents evoked at −80 mV in MmPiezo1-transfected cells and fitted with a Boltzmann equation. Each data point is the mean ± s.e.m. of 3–13 observations. **d**, Representative traces of Piezo-dependent mechanically activated currents evoked at −80 mV in the presence of ruthenium red. **e**, Blocking effect of ruthenium red on Piezo-dependent mechanically activated currents evoked at −80 mV. Bars represent mean ± s.e.m. and the number of cells tested is shown above the bars. **$P < 0.01$; ***$P < 0.001$; unpaired *t*-test.

outwards currents. Such voltage dependence is a characteristic of open channel block. A high concentration of ruthenium red (50 µM) included in the pipette solution in the whole-cell configuration showed no evidence of block, as large mechanically activated currents still displayed a linear *I*–*V* relationship (Supplementary Fig. 2). These results suggest that ruthenium red blocks the pore of MmPiezo1-induced mechanically activated channels from the extracellular side. Notably, DmPiezo-induced mechanically activated currents were insensitive to ruthenium red concentrations that potently blocked MmPiezo1-induced currents (Fig. 2d, e). Together, these results demonstrate that overexpression of DmPiezo or MmPiezo1 gives rise to mechanically activated channels with distinct channel properties.

Next, we set out to determine the single channel conductance (γ) of mechanically activated channels induced by Piezo proteins by using negative-pressure stimulations of membrane patches in cell-attached mode. Figure 3 shows the single mechanically activated channel properties of MmPiezo1 or DmPiezo. Openings of stretch-activated channels showed a marked difference in amplitude of single channel currents (Fig. 3a), as determined from the single channel *I*–*V* relationship for MmPiezo1 and DmPiezo (Fig. 3b, c). Linear regression of these *I*–*V* relationships resulted in slope-conductance values in these recording conditions of 29.9 ± 1.9 and 3.3 ± 0.3 pS for MmPiezo1- and DmPiezo-induced mechanically activated currents, respectively ($n = 7$ and 5 cells; mean ± s.e.m.). Therefore, DmPiezo-dependent channels are ninefold less conductive than MmPiezo1-dependent channels.

MmPiezo1 oligomerization

The pore of most ion channels is formed by the assembly of transmembrane domains from distinct subunits (for example, voltage-gated K^+ channels, ligand-gated ion channels) or structurally repetitive domains within a large protein (for example, voltage gated Na^+ and Ca^{2+} channels). As Piezo proteins lack repetitive transmembrane motifs presumably they oligomerize to form ion channels. To test this hypothesis, we determined the number of subunits in Piezo complexes by expressing GFP–MmPiezo1 fusion proteins in *Xenopus laevis* oocytes, imaging individual spots with total internal reflection microscopy (TIRF), and counting discrete photobleaching steps (Fig. 4a, b and ref. 22). Amino-terminal GFP–MmPiezo1 functionality was confirmed by overexpression in HEK293T cells (Supplementary Fig. 3). We used several GFP fusion constructs of ion channels with known stoichiometry as controls: voltage-gated Ca^{2+} channel (α1E–GFP; monomer), NMDA (*N*-methyl-D-aspartate) receptor (NR1 co-expressed with NR3A–GFP; dimer of dimers) and cyclic nucleotide gated (CNG) channel (XfA4–GFP; tetramer)[22]. We found that complexes of MmPiezo1 frequently exhibited at most four photobleaching steps, consistent with the idea that Piezo proteins homo-multimerize. Fluorescent MmPiezo1 (or CNG) complexes exhibiting bleaching in fewer than four steps can be explained by non-functional GFP or pre-bleached GFP[22] or general bias against noisier multi-step traces during data analysis (see Methods). Histograms of the number of photobleaching steps observed for MmPiezo1 complexes were comparable to histograms obtained from tetrameric CNG channels (Fig. 4c). These results suggest that in living cells, Piezo proteins can assemble as homo-multimers.

We further characterized Piezo proteins biochemically by heterologously expressing and purifying MmPiezo1 carboxy-terminally fused with a glutathione *S*-transferase (MmPiezo1–GST). Functionality of MmPiezo1–GST was confirmed by overexpression in HEK293T cells (Supplementary Fig. 3). We observed a protein band at a position near the 260-kDa protein marker on a Coomassie-blue-stained denaturing protein gel (Supplementary Fig. 4a). Western blot with a GST (*Schistosoma japonicum* form) antibody (Supplementary Fig. 4b) or

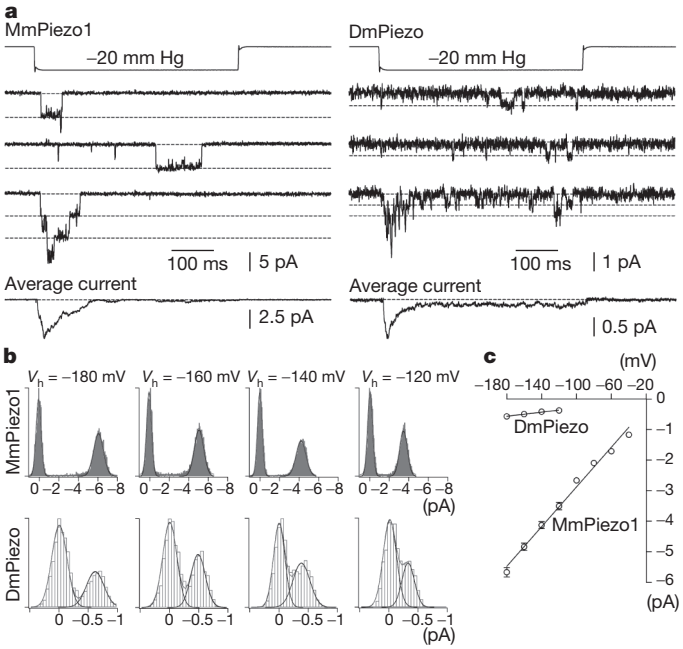

Figure 3 | MmPiezo1- and DmPiezo-induced stretch-activated channels have different conductances. **a**, Representative Piezo-dependent stretch-activated channel openings elicited at −180 mV. Bottom traces represent average of 40 individual recording traces. **b**, All-point histograms of single channel opening events (average of 10 and 20 individual events for MmPiezo1 and DmPiezo, respectively) at different holding potentials (V_h). **c**, Average *I–V* relationships of stretch activated single channels in MmPiezo1 and DmPiezo transfected cells ($n = 7$ and 5 cells, respectively; mean ± s.e.m.). Single channel amplitude was determined as the amplitude difference in Gaussian fits as shown in **b**.

a MmPiezo1-specific antibody[8] (Fig. 4) confirmed the presence of MmPiezo1–GST in the MmPiezo1–GST sample. Using native gel electrophoresis and Coomassie blue staining, we detected a prominent protein band at a position near the 1,236 kDa protein marker only in the MmPiezo1–GST sample (Fig. 4d). Western blot using MmPiezo1 antibody confirmed that this major band contains MmPiezo1 (Fig. 4e). These data indicate that the purified MmPiezo1–GST protein complex has a molecular weight of about 1.2 million Da, four times the predicted molecular weight of a single MmPiezo1–GST polypeptide (318 kDa). Next, we asked whether any endogenous proteins are present in this MmPiezo1-containing complex. Mass spectrometry of the ~1.2 million Da protein complex mainly detected peptides derived from MmPiezo1–GST, but not from other endogenous membrane proteins. Although several non-transmembrane proteins were also detected, most of them were also present in the control sample, indicating an absence of specific interacting proteins in the complex (Supplementary Table 1). Moreover, mass spectrometry of the whole purified solution samples before gel electrophoresis confirmed that no other ion channel protein was detected (Supplementary Table 2). This indicates that MmPiezo1 is not tightly associated with any endogenous pore-forming protein.

To examine further whether this Piezo complex is indeed a tetramer, we treated the purified MmPiezo1–GST protein with the crosslinker formaldehyde and subjected the samples to denaturing gel electrophoresis and western blotting. Formaldehyde-treated samples contained three major additional higher-order Piezo-containing bands, with longer treatments increasing the prominence of the higher bands (Fig. 4f). The distribution of the bands on the 3–8% gradient gel suggests that the four bands correspond to monomer, dimer, trimer and tetramer of MmPiezo1–GST (Fig. 4f). The observation that MmPiezo1 is crosslinked by formaldehyde, a crosslinker with a relative short spacer arm (2.3–2.7 Å), suggests that the subunits form a tetramer.

It is possible that MmPiezo1 oligomers associate with other proteins; however, such an association might not withstand the GST purification step. To probe this, we performed paraformaldehyde (PFA) crosslinking experiments on living cells before the purification procedure. On a native gel, the MmPiezo1–GST complex purified from PFA-treated cells also migrated to the position near the 1,236 kDa protein marker, similar to the sample from untreated cells (Fig. 4g). On a denaturing gel, on-cell PFA treatment resulted in four distinct MmPiezo1-specific bands, similar to results of formaldehyde treatment on the purified complex (Fig. 4h). This suggests that MmPiezo1 is not tightly associated with other proteins large enough to alter discernibly its size on denaturing gels, and confirms the results from mass spectrometry analysis. However, our crosslinking studies with PFA might miss weak interactors with MmPiezo1. Regardless, together with the results obtained from single-molecule photobleaching analysis in living cells, our biochemical data suggest that MmPiezo1 forms a homomultimeric ion channel, most likely as a homotetramer.

MmPiezo1 reconstitution in lipid bilayers

Finally, to assess whether Piezo proteins were sufficient to recapitulate the channel properties recorded from Piezo-overexpressing cells, we reconstituted purified MmPiezo1 proteins into lipid bilayers in two distinct configurations: droplet interface lipid bilayers (DIBs) assembled from two monolayers[23–25] (Fig. 5a–e and l–q) and proteoliposomes[26] (Fig. 5f–h). In the first configuration, MmPiezo1 was reconstituted into asymmetric bilayers that mimic the cellular environment: the extracellular-facing lipid monolayer is predominantly neutral whereas the intracellular-facing leaflet is negatively charged[27]. In contrast, the lipid composition of the bilayer in the second configuration is uniform.

In the DIBs setting, representative segments from a 6-min recording obtained at −100 mV show brief, discrete channel openings (Fig. 5a, b) blocked by addition of 50 μM ruthenium red to the neutral facing compartment (Fig. 5c). In contrast, no effect was observed when ruthenium red was introduced into the negative-facing compartment (not shown). We detected efficient block of channel activity even at 5 μM ruthenium red (not shown). The asymmetric accessibility of ruthenium red block of reconstituted channels agrees with the data obtained from MmPiezo1-overexpressing HEK293T cells (Fig. 2 and Supplementary Fig. 2), thereby establishing the fidelity of the assays and validating MmPiezo1 protein as an authentic ion channel. The Piezo currents exhibit ohmic behaviour; records displayed at higher resolution (Fig. 5b) clearly demonstrate the occurrence of unitary events with γ values obtained from conductance histograms of 118 ± 15 pS and 80 ± 6 pS ($n = 6$) in symmetric 0.5 M KCl from the negative and positive branches of *I–V* plots, respectively (Fig. 5d, e).

A similar pattern of activity was obtained from MmPiezo1 reconstituted in asolectin liposomes[26] (Fig. 5f–k). A selection of recordings shows the presence of two channels in the membrane which reside predominantly in the open state (Fig. 5f, g), as discerned in a higher time resolution display (Fig. 5k). These recordings were obtained in the presence of 50 μM ruthenium red inside the recording pipette, to ensure functional selection of a single population of MmPiezo1 channels facing the ruthenium-red-free compartment. MmPiezo1 in asolectin proteoliposomes under these conditions (symmetric 0.2 M KCl) exhibits a $\gamma = 110 \pm 10$ pS at $V = -100$ mV and 80 ± 5 pS at $V = 100$ mV (Fig. 5h–j) ($n = 8$). Finally, reconstitution of control samples purified from non-transfected cells as well as heat-denatured purified MmPiezo1–GST into either bilayer systems under otherwise identical conditions failed to reproduce this pattern of channel activity (not shown).

We then tested the ability of the reconstituted MmPiezo1 to conduct sodium (Fig. 5l-q). Initially, single channel currents were recorded from asymmetric bilayers in symmetric 0.2 M KCl; $\gamma = 58 \pm 5$ pS (Fig. 5l, o). Subsequent addition of 0.2 M NaCl in the presence of 0.2 M KCl increased the unitary conductance of reconstituted channels to 95 ± 5 pS (Fig. 5m, p) while retaining sensitivity to ruthenium red

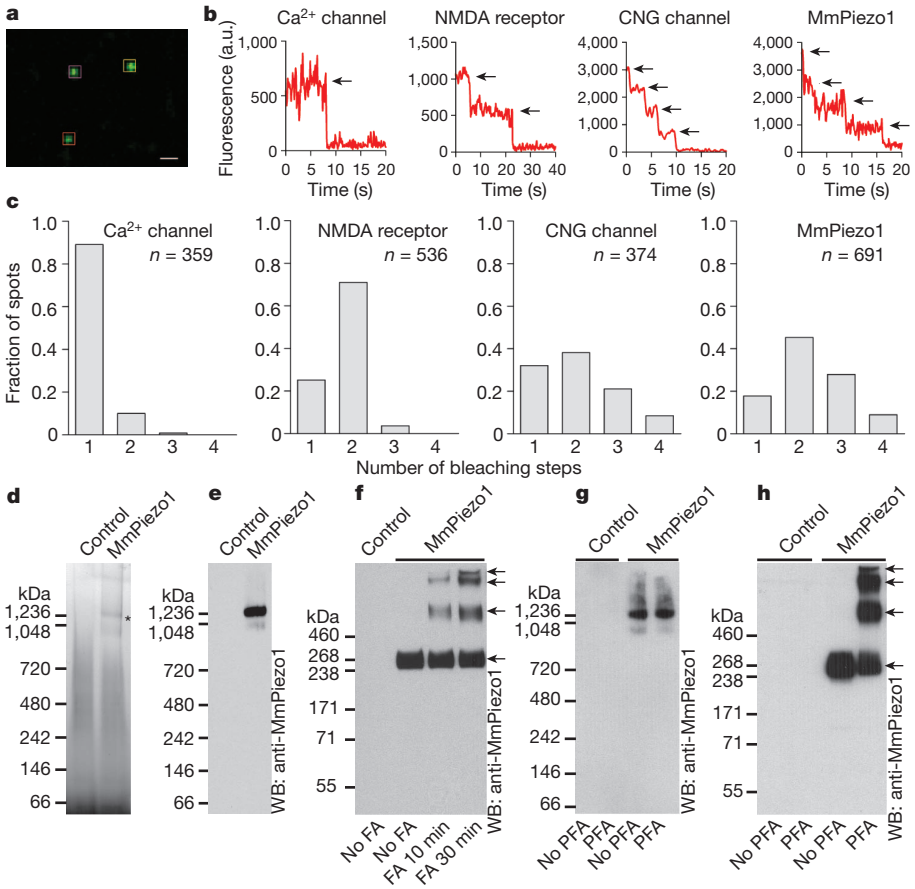

Figure 4 | MmPiezo1 forms homo-oligomers. **a**, Representative image of an acquired sequence showing three selected GFP–MmPiezo1 spots in the cell membrane. Levels were adjusted for clarity. Scale bar, 0.8 μm. **b**, Representative traces of fluorescence intensities of indicated single GFP-fusion constructs. Black arrows indicate photobleaching steps. **c**, Histograms of the average number of bleaching steps observed in ten or more movies from four or more oocytes of single fluorescent complexes of indicated constructs. **d**, **e**, Indicated samples purified and separated on native gels and visualized by Coomassie staining (**d**) or western blotting (**e**). Asterisk in **d** indicates a protein band specifically present in the MmPiezo1 sample. **f**, Purified MmPiezo1–GST proteins treated with or without formaldehyde (FA) with the indicated time period, separated on a denaturing gel and detected with the anti-MmPiezo1 antibody. Sample purified from cells without transfection served as a negative control. **g**, **h**, MmPiezo1–GST-transfected HEK293T cells or untransfected cells treated with or without 0.25% PFA for 10 min. The crosslinked MmPiezo1–GST proteins were purified and separated on native gel (**g**) or denaturing gels (**h**), followed by western blotting. Panels **d**–**h** are representatives of at least three independent experiments.

block (Fig. 5n, q). These results confirm that these channels conduct both sodium and potassium as would be expected from a cationic non-selective channel. This assertion was further substantiated by recording MmPiezo1 currents from proteoliposomes under bi-ionic conditions (0.2 M KCl/0.2 M NaCl) (Supplementary Fig. 5a–h). A summary of the $I-V$ relation for the MmPiezo1 channel, extracted from 204,088 events obtained in three experiments, shows that the single channel current is ohmic between −100 and 200 mV with a slope conductance of 102 ± 2 pS (Supplementary Fig. 5i). The current reversed direction at 0.0 ± 0.3 mV, demonstrating that the channel does not select between K^+ and Na^+, and importantly, displays open channel block by ruthenium red (Supplementary Fig. 5j–l).

The difference in γ between overexpressed MmPiezo1 in cells and reconstituted MmPiezo1 in lipid bilayers may be attributed to many variables, including the distinct lipid environments which are known to influence conductance measurements strongly[28–32]. Moreover, the ionic conditions used in the two systems are different, as divalent cations present in HEK293T cell-attached experiments also affect the conductance values. Indeed, when divalent cations are excluded from the recording pipette, γ of MmPiezo1-induced currents in HEK293T cells is 58.0 pS ± 1.5 pS (150 mM NaCl solution, Supplementary Fig. 6), compared to 29.9 ± 1.5 pS in the presence of divalent ions (Fig. 3). The near equivalence of γ values together with the similar pattern of channel activity demonstrates that reconstitution of MmPiezo1 into two distinct bilayer systems produces channels with identical functional properties (Supplementary Table 3).

Future reconstitution and recording of DmPiezo in lipid bilayers will show whether the difference in conductance between MmPiezo1 and DmPiezo arises from intrinsic properties. The membrane environment and lipid composition are known to modulate the activity of the embedded channel proteins in a drastic and deterministic manner (for example, see refs 28–32). It is not entirely surprising that the conditions to emulate the cellular environment in the reconstituted system in terms of the mechanical state of the membrane or its lipid composition have thus far been inadequate to retrieve the activation features of mechanically activated ion channels. Furthermore, the complexity of protein clusters and dynamic cytoskeletal interacting partners at the cell membrane[33] introduce regulatory constraints on channel activity. Further investigation may clarify whether Piezo ion channel subunits are intrinsically mechanosensitive or use unknown interacting partners to sense membrane tension.

Concluding remarks

We provide compelling evidence to support the hypothesis that Piezo proteins are indeed ion channels. First, overexpression of DmPiezo or MmPiezo1 in a human cell line gives rise to mechanically activated channels with distinct biophysical and pore-related properties. Second, isolated Piezo complexes do not contain detectable amounts

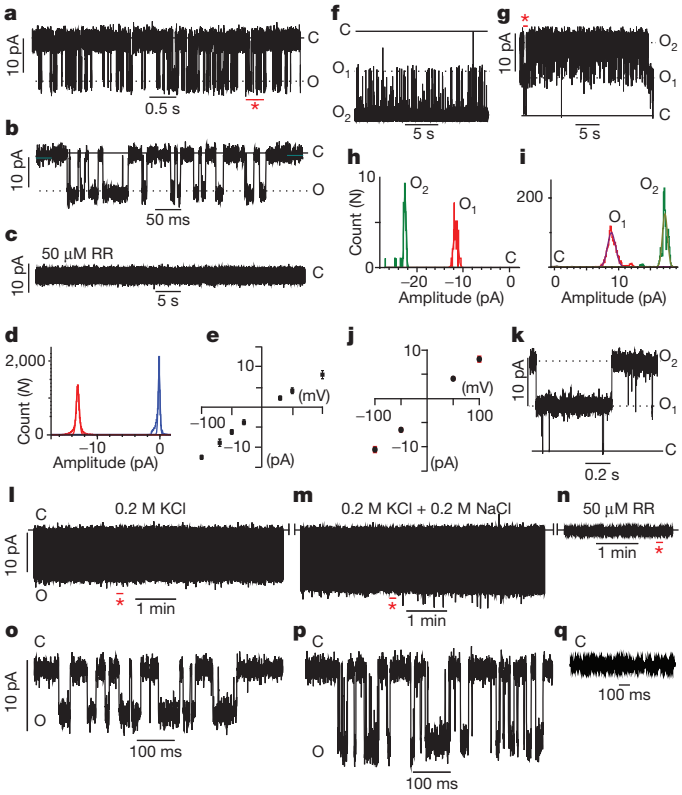

Figure 5 | MmPiezo1 forms ruthenium-red-sensitive ion channels. **a**–**e**, Reconstitution of purified MmPiezo1 into asymmetric lipid bilayers. **a**, Representative single channel currents at −100 mV. The section of the recordings indicated by the red asterisk is shown in **b** at a 10-fold higher time resolution. **c**, After 35 min of recording the channel activity shown in **a**, injection of 50 μM ruthenium red onto the neutral facing compartment blocks MmPiezo1 currents. **d**, All-event current amplitude histogram of a 6-min recording; $\gamma = 124 \pm 7$ pS. The total number of opening events (N) analysed was 18,424. **e**, Single channel I–V relationship, $n = 6$ experiments. **f**–**k**, Reconstitution of purified MmPiezo1 into asolectin proteoliposomes. Representative channel currents recorded at −100 mV (**f**) and +100 mV (**g**) in the presence of 50 μM ruthenium red inside the recording pipette. Two open channels are present in the membrane. The segment of the 15 min recording shown in **g** indicated by the red asterisk is displayed in **k** at a 25-fold higher time resolution. **h**, **i**, All-event current amplitude histograms from 30 s (**h**) and 15 min (**i**) recordings: $\gamma = 110 \pm 10$ pS (**h**) and 80 ± 5 pS (**i**); N was 9,938 events. **j**, Single channel I–V relationship, $n = 8$ experiments. **l**–**q**, Representative single channel currents at −100 mV of purified MmPiezo1 reconstituted into asymmetric lipid bilayers in symmetric 0.2 M KCl (**l**), after addition of 0.2 M NaCl (**m**) and after addition of 50 μM ruthenium red (**n**). Segments indicated by red asterisks in **l**–**n** are displayed in panels **o**–**q**, respectively. C and O denote the closed and open states.

of other channel-like proteins. Finally, purified MmPiezo1 protein reconstituted into proteoliposomes and planar lipid bilayers in the absence of any other cellular components gives rise to ruthenium-red-sensitive cationic ion channel activity. The MmPiezo1 complex is estimated to weigh ~1.2-million Da with 120–160 transmembrane segments, being, to our knowledge, the largest plasma membrane ion channel complex identified so far.

METHODS SUMMARY

Electrophysiology. Mechanical stimulation was achieved as previously described[8].

Subunit counting. The preparations were imaged on an inverted Nikon Ti-E fluorescence TIRF microscope (Nikon Corporation) and imaged with a high numerical aperture objective (Nikon ×100 PlanApo, NA1.49). eGFP-fusion proteins were excited with a 488-nm Coherent laser (Coherent, Inc.) and images were collected with an Andor iXon DU-897 EMCCD camera.

MmPiezo1–GST purification. Cells were collected and lysed 24 h after transfection, followed by an affinity purification. Initially, purification was conducted from whole-cell lysates. Thereafter, purification was performed using the membrane fraction as starting material, resulting in significantly enhanced frequency of retrieval of channel activity after reconstitution. Untransfected cells were subjected to the same purification procedure to serve as a negative control. Purified samples were kept at 4 °C until further analysis.

Native gel electrophoresis. The purified MmPiezo1–GST proteins or negative control samples were subjected to 3–12% NativePAGE Novex Bis-Tris gel for native (non-denaturing) electrophoresis according to the user manual (Invitrogen). After electrophoresis, the native gel was then either visualized by a fast Coomassie G-250 staining or transferred to a PVDF membrane for western blotting.

Reconstitution in lipid bilayers and proteoliposomes. Purified MmPiezo1 was reconstituted into proteoliposomes by detergent dilution. Excised patches from giant asolectin proteoliposomes were used for channel recordings. Asymmetric lipid bilayers were formed using the droplet interface strategy; one monolayer was composed of 1,2-diphytanoyl-*sn*-glycero-3 phosphocholine (DPhPC), and the other of 90% DPhPC and 10% of the negatively charged lipid, 1,2-dioleoyl-*sn*-glycero-3-phosphatidic acid (DOPA) (mole/mole) (Avanti Polar Lipids).

Full Methods and any associated references are available in the online version of the paper at www.nature.com/nature.

Received 22 July; accepted 21 December 2011.
Published online 19 February 2012.

1. Corey, D. P. & Hudspeth, A. J. Response latency of vertebrate hair cells. *Biophys. J.* **26,** 499–506 (1979).
2. McCarter, G. C., Reichling, D. B. & Levine, J. D. Mechanical transduction by rat dorsal root ganglion neurons *in vitro*. *Neurosci. Lett.* **273,** 179–182 (1999).
3. Davis, M. J., Donovitz, J. A. & Hood, J. D. Stretch-activated single-channel and whole cell currents in vascular smooth muscle cells. *Am. J. Physiol.* **262,** C1083–C1088 (1992).
4. Praetorius, H. A. & Spring, K. R. Bending the MDCK cell primary cilium increases intracellular calcium. *J. Membr. Biol.* **184,** 71–79 (2001).
5. Chalfie, M. Neurosensory mechanotransduction. *Nature Rev. Mol. Cell Biol.* **10,** 44–52 (2009).
6. Delmas, P., Hao, J. & Rodat-Despoix, L. Molecular mechanisms of mechanotransduction in mammalian sensory neurons. *Nature Rev. Neurosci.* **12,** 139–153 (2011).
7. Hamill, O. P. & Martinac, B. Molecular basis of mechanotransduction in living cells. *Physiol. Rev.* **81,** 685–740 (2001).
8. Coste, B. *et al.* Piezo1 and Piezo2 are essential components of distinct mechanically activated cation channels. *Science* **330,** 55–60 (2010).
9. Bae, C., Sachs, F. & Gottlieb, P. A. The mechanosensitive ion channel Piezo1 is inhibited by the peptide GsMTx4. *Biochemistry* **50,** 6295–6300 (2011).
10. Reed-Geaghan, E. G. & Maricich, S. M. Peripheral somatosensation: a touch of genetics. *Curr. Opin. Genet. Dev.* **21,** 240–248 (2011).
11. Nilius, B. Pressing and squeezing with Piezos. *EMBO Rep.* **11,** 902–903 (2010).
12. Gong, Z. *et al.* Two interdependent TRPV channel subunits, inactive and Nanchung, mediate hearing in *Drosophila*. *J. Neurosci.* **24,** 9059–9066 (2004).
13. Kim, J. *et al.* A TRPV family ion channel required for hearing in *Drosophila*. *Nature* **424,** 81–84 (2003).
14. Tracey, W. D. Jr, Wilson, R. I., Laurent, G. & Benzer, S. *painless*, a *Drosophila* gene essential for nociception. *Cell* **113,** 261–273 (2003).
15. Walker, R. G., Willingham, A. T. & Zuker, C. S. A *Drosophila* mechanosensory transduction channel. *Science* **287,** 2229–2234 (2000).
16. Zhong, L., Hwang, R. Y. & Tracey, W. D. Pickpocket is a DEG/ENaC protein required for mechanical nociception in *Drosophila* larvae. *Curr. Biol.* **20,** 429–434 (2010).
17. Coste, B., Crest, M. & Delmas, P. Pharmacological dissection and distribution of NaN/Nav1.9, T-type Ca^{2+} currents, and mechanically activated cation currents in different populations of DRG neurons. *J. Gen. Physiol.* **129,** 57–77 (2007).
18. Drew, L. J., Wood, J. N. & Cesare, P. Distinct mechanosensitive properties of capsaicin-sensitive and -insensitive sensory neurons. *J. Neurosci.* **22,** RC228 (2002).
19. Kim, S. E., Coste, B., Chadha, A., Cook, B. & Patapoutian, A. The role of *Drosophila* Piezo in mechanical nociception. *Nature* http://dx.doi.org/10.1038/nature10801 (this issue).
20. Voets, T. *et al.* Molecular determinants of permeation through the cation channel TRPV4. *J. Biol. Chem.* **277,** 33704–33710 (2002).
21. Voets, T. *et al.* TRPM6 forms the Mg^{2+} influx channel involved in intestinal and renal Mg^{2+} absorption. *J. Biol. Chem.* **279,** 19–25 (2004).
22. Ulbrich, M. H. & Isacoff, E. Y. Subunit counting in membrane-bound proteins. *Nature Methods* **4,** 319–321 (2007).
23. Bayley, H. *et al.* Droplet interface bilayers. *Mol. Biosyst.* **4,** 1191–1208 (2008).
24. Montal, M. Asymmetric lipid bilayers. Reponse to multivalent ions. *Biochim. Biophys. Acta* **298,** 750–754 (1973).
25. Montal, M. & Mueller, P. Formation of bimolecular membranes from lipid monolayers and a study of their electrical properties. *Proc. Natl Acad. Sci. USA* **69,** 3561–3566 (1972).
26. Santos, J. S., Grigoriev, S. M. & Montal, M. Molecular template for a voltage sensor in a novel K^+ channel. III. Functional reconstitution of a sensorless pore module from a prokaryotic Kv channel. *J. Gen. Physiol.* **132,** 651–666 (2008).
27. Leventis, P. A. & Grinstein, S. The distribution and function of phosphatidylserine in cellular membranes. *Annu Rev Biophys* **39,** 407–427 (2010).

28. Ermakov, Y. A., Kamaraju, K., Sengupta, K. & Sukharev, S. Gadolinium ions block mechanosensitive channels by altering the packing and lateral pressure of anionic lipids. *Biophys. J.* **98,** 1018–1027 (2010).
29. Gambale, F. & Montal, M. Characterization of the channel properties of tetanus toxin in planar lipid bilayers. *Biophys. J.* **53,** 771–783 (1988).
30. Oliver, D. *et al.* Functional conversion between A-type and delayed rectifier K^+ channels by membrane lipids. *Science* **304,** 265–270 (2004).
31. Schmidt, D. & MacKinnon, R. Voltage-dependent K^+ channel gating and voltage sensor toxin sensitivity depend on the mechanical state of the lipid membrane. *Proc. Natl Acad. Sci. USA* **105,** 19276–19281 (2008).
32. Tao, X. & MacKinnon, R. Functional analysis of Kv1.2 and paddle chimera Kv channels in planar lipid bilayers. *J. Mol. Biol.* **382,** 24–33 (2008).
33. Hartman, N. C. & Groves, J. T. Signaling clusters in the cell membrane. *Curr. Opin. Cell Biol.* **23,** 370–376 (2011).

Supplementary Information is linked to the online version of the paper at www.nature.com/nature.

Acknowledgements We thank M. H. Ulbrich for providing Ca^{2+} channel-, NMDA receptor- and CNG channel–GFP fusion constructs used as controls for photobleaching experiments. This research was supported by grants from the National Institutes of Dental and Craniofacial Research, Neurological Disorders, General Medical Sciences, and by The Genomics Institute of the Novartis Research Foundation. B.X. and J.G. are postdoctoral fellowship recipients from the American Heart Association and the NIH, respectively.

Author Contributions B.C. performed and analysed electrophysiological experiments. B.X. performed and analysed biochemical experiments. J.S.S. and R.S. performed the reconstitution experiments and together with M.M. analysed the single channel data. J.G. and K.S.S. performed and analysed photo-bleaching experiments. S.E.K. cloned the Dm*piezo* gene. M.S. initiated biochemical experiments. J.M. generated GFP-Mm*Piezo1* and the mRNA used for oocyte injection. A.E.D. provided technical help for oocyte experiments. A.P., B.C., B.X., J.G., J.S.S., R.S., and M.M. wrote the manuscript.

Author Information The DmPiezo sequence has been deposited in GenBank under accession number JQ425255. Reprints and permissions information is available at www.nature.com/reprints. The authors declare no competing financial interests. Readers are welcome to comment on the online version of this article at www.nature.com/nature. Correspondence and requests for materials should be addressed to A.P. (apatapou@gnf.org) and M.M. (mmontal@ucsd.edu).

METHODS

Cloning of *Drosophila piezo* full-length cDNA. The *Drosophila piezo* gene (GenBank accession number JQ425255) was cloned from adult *Drosophila* poly(A)$^+$ RNAs (Clonetech) by RT–PCR. Primers for RT–PCR were designed based on the annotated sequence of CG8486. Two fragments of 2 kb and 6.5 kb were amplified and cloned sequentially into pIRES2-EGFP expression vector. Each cloning step was sequence verified. Full-length *Drosophila piezo* gene is 8,355 bp in length. The protein sequence of DmPiezo is shown in Supplementary Fig. 1.

Cell culture and transient transfection. Human embryonic kidney 293T (HEK293T), NIH-3T3, F11 and HeLa cells were grown in Dulbecco's Modified Eagle Medium containing 4.5 mg ml^{-1} glucose, 10% fetal bovine serum, 50 U ml^{-1} penicillin and 50 μg ml^{-1} streptomycin. Cells were plated onto poly-lysine-coated 12-mm round glass coverslips placed in 24-well plates and transfected using lipofectamine 2000 (Invitrogen) according to the manufacturer's instruction. 500–1,000 ng ml^{-1} of plasmid DNA was transfected and cells were recorded 12–48 h later.

Electrophysiology. Patch-clamp experiments were performed in standard whole-cell or cell-attached recordings using an Axopatch 200B amplifier (Axon Instruments). Patch pipettes had resistance of 2–3 MΩ when filled with an internal solution consisting of (in mM) 133 CsCl, 10 HEPES, 5 EGTA, 1 $CaCl_2$, 1 $MgCl_2$, 4 MgATP and 0.4 Na_2GTP (pH adjusted to 7.3 with CsOH). The extracellular solution consisted of (in mM) 130 NaCl, 3 KCl, 1 $MgCl_2$, 10 HEPES, 2.5 $CaCl_2$, 10 glucose (pH adjusted to 7.3 with NaOH). For cell-attached recordings, pipettes were filled with a solution consisting of (in mM) 130 NaCl, 5 KCl, 10 HEPES, 1 $CaCl_2$, 1 $MgCl_2$, 10 TEA-Cl (pH 7.3 with NaOH), except for Supplementary Fig. 6 where the internal solution was (in mM) 150 NaCl, 10 HEPES (pH adjusted to 7.3 with NaOH). External solution used to zero the membrane potential consisted of (in mM) 140 KCl, 10 HEPES, 1 $MgCl_2$, 10 glucose (pH 7.3 with KOH). All experiments were done at room temperature. Currents were sampled at 50 or 20 kHz and filtered at 5 or 2 kHz. Voltages were not corrected for a liquid junction potential. Leak currents before mechanical stimulations were subtracted off-line from the current traces. 10 mM ruthenium red stock solution was prepared in water.

Mechanical stimulation. For whole-cell recordings mechanical stimulation was achieved using a fire-polished glass pipette (tip diameter 3–4 μm) positioned at an angle of 80° to the cell being recorded. Downward movement of the probe towards the cell was driven by a Clampex controlled piezo-electric crystal microstage (E625 LVPZT Controller/Amplifier; Physik Instrumente). The probe was typically positioned ~2 μm from the cell body. The probe had a velocity of 1 μm ms^{-1} during the ramp segment of the command for forward motion and the stimulus was applied for 150 ms. To assess the mechanical sensitivity of a cell, a series of mechanical steps in 1 μm increments was applied every 10–20 s, which allowed full recovery of mechanosensitive currents. Inward mechanically activated currents were recorded at a holding potential of −80 mV. For *I–V* relationship recordings, voltage steps were applied 0.7 s before the mechanical stimulation from a holding potential of −60 mV.

For cell-attached recordings, membrane patches were stimulated with brief negative pressure pulses through the recording electrode using a Clampex controlled pressure clamp HSPC-1 device (ALA-scientific). Unless otherwise stated, stretch-activated channels were recorded at a holding potential of −80 mV with pressure steps from 0 to −60 mmHg (−10 mm Hg increments). Current–pressure relationships were fitted with a Boltzmann equation of the form: $I(P) = [1 + \exp(-(P - P_{50})/s)]^{-1}$, where I is the peak of stretch-activated current at a given pressure, P is the applied patch pressure (in mm Hg), P_{50} is the pressure value that evoked a current value which is 50% of I_{max}, and s reflects the current sensitivity to pressure.

Single-channel amplitude characterization was performed on patches that showed strong stretch-activated current activity at −80 mV using increasing steps of negative pressure up to −60 mm Hg. Similar activity was never present in control-transfected cells. Negative pressure steps were then reduced to low to moderate level (−5 to −20 mm Hg) allowing detection of single channel openings.

Subunit counting. For oocyte injection, all construct plasmids were linearized at C terminus with NheI, HindIII or NotI and DNA transcribed with T7 mMessage mMachine Kit (Ambion) and poly(A)-tailing Kit (Ambion) and cleaned with LiCl precipitation. 50 nl of 0.2 μg μl^{-1} mRNA was injected into *Xenopus* oocytes (Nasco).

For acquisition, 12–24 h after injection, oocytes were osmotically shocked in stripping buffer (in mM: 220 *N*-methyl glucamine aspartate, 10 HEPES, 1 $MgCl_2$) and mechanically de-vitellinated. MatTek dishes (MatTek Corporation) were prepared by sonication in 1 M KOH to remove background fluorescence and further sonicated in MilliQ dH_2O. Oocytes were placed onto MatTek dishes into SOS buffer (in mM: 100 NaCl, 2 KCl, 1.8 $CaCl_2$-H_2O, 1 $MgCl_2$-$6H_2O$, 5 HEPES, 2.5 Na pyruvate and 50 μg ml^{-1} gentamicin, pH 7.0). The preparations were imaged on an inverted Nikon Ti-E fluorescence TIRF microscope (Nikon Corporation) and imaged with a high numerical aperture objective (Nikon 100× PlanApo, NA1.49) with an additional ×1.5 Optovar magnification. eGFP fusion proteins were excited with a 488-nm Coherent laser (Coherent, Inc.) and images were collected with an Andor iXon DU-897 EMCCD camera. Sixty-second movies were collected at 100-ms exposures, for a frame rate of 10 Hz.

Using Nikon Elements software, movies were duplicated and processed with a rolling average of 2. A second duplicate was filtered with a low-pass kernel of 7, to remove background. The low-pass images were subtracted from the averaged images, to produce the movies used for analysis. Non-overlapping 4 × 4 pixel regions of interest were drawn around randomly selected spots that were clearly separated from neighbouring bright pixels. The spots were required to fit entirely within the 4 × 4 pixel regions. Pixel size was 0.11 μm. The average intensity of each region was plotted over the length of the movies. Traces were discarded if the intensity increased after an initial decrease, if the fluorescent spot moved out of the region, or if the fluorescent signal showed a continuous decay instead of stepwise bleaching. Finally, the number of bleaching steps was counted for each spot.

MmPiezo1–GST purification. The MmPiezo1–GST construct was subcloned by inserting a GST encoding sequence from *Schistosoma japonicum* into the MmPiezo1 construct[8] at the 3′ end of MmPiezo1 cDNA sequence using the AscI and SacII restriction enzyme sites. The resulting MmPiezo1–GST fusion protein has 2,773 amino acids.

After incubation with cell lysates overnight at 4 °C, the glutathione beads were washed four times in a buffer containing 25 mM NaPIPES, 140 mM NaCl, 0.6% CHAPS, 0.14% phosphatidylcholine (PC), 2.5 mM dithiothreitol (DTT), and a cocktail of protease inhibitors and eluted with 100 mM glutathione in a buffer containing 25 mM NaPIPES, 50 mM Tris, 0.6% CHAPS, 0.14% PC, 2.5 mM DTT and a cocktail of protease inhibitors. The eluant was dialysed against a buffer containing 25 mM NaPIPES, 0.6% CHAPS, 0.14% PC, 2.5 mM DTT and a cocktail of protease inhibitors. The purified samples were kept at 4 °C. Samples purified according to this protocol were used for all the biochemical work and the initial reconstitution experiments. However, because retrieval of channel activity from the reconstituted MmPiezo1–GST fluctuated from preparation to preparation, we adopted an alternative purification protocol involving the membrane fraction as the starting material. Specifically, 24 h after transfection, cells were collected and homogenized in a buffer containing 25 mM NaPIPES, 50 mM NaCl, 2.5 mM DTT, and a cocktail of protease inhibitors. The cell suspension was forced to go through a 25.5 G needle for 20 times and centrifuged at 1,000*g* for 15 min at 4 °C. The supernatant was collected and centrifuged at 167,000*g* for 30 min at 4 °C. The resulting membrane fraction was washed three times (using a buffer containing 25 mM NaPIPES, 150 mM NaCl, 2.5 mM DTT, and a cocktail of protease inhibitors) and used as the starting material for MmPiezo1–GST purification using the same procedure described above. Purification from the membrane fraction greatly reduced the content of endogenous GST proteins and significantly enhanced the frequency of retrieval of MmPiezo1 channel activity after reconstitution (Fig. 5, Supplementary Fig. 5 and Supplementary Table 3).

NativePAGE Novex Bis-Tris gel. The purified MmPiezo1–GST proteins and control samples were subjected to 3–12% NativePAGE Novex Bis-Tris gel for native (non-denaturing) electrophoresis according to the User Manual (Invitrogen). In brief, samples were mixed with NativePAGE Sample Buffer and NativePAGE 5% G-250 Sample Additive and then subjected to electrophoresis at 150 V for 2 h. The use of G-250 charge-shift in NativePAGE gels results in protein resolution based upon protein size and therefore allows accurate size estimation of native protein complexes[34]. However, the native protein conformation may give an expected size estimation error of ~15%. After electrophoresis, the native gel was then either visualized by a fast Coomassie G-250 staining or transferred to a PVDF membrane for western blotting with an antibody specifically against Piezo1 proteins.

Formaldehyde and paraformaldehyde crosslinking. The purified MmPiezo1–GST proteins were treated with or without 0.1% formaldehyde at room temperature for different periods of time and then mixed with NuPAGE LDS Sample Buffer and NuPAGE Reducing Agent (Invitrogen), followed by heating at 70 °C for 10 min to denature the protein. The treated samples were subjected to 3–8% NuPAGE Tris-Acetate gel electrophoresis under denaturing conditions. For live cell crosslinking, 0.25% concentration of PFA was added to the cell culture medium and kept at room temperature for 10 min, followed by adding 125 mM glycine to stop the PFA crosslinking reaction. Treated cells were collected and subjected to sequential steps of protein purification, 3–8% NuPAGE Tris-Acetate gel electrophoresis under denaturing conditions or 3–12% NativePAGE Novex Bis-Tris gel for native (non-denaturing) electrophoresis, and western blotting with the anti-Piezo1 antibody.

Western blotting. After electrophoresis, either the native or denaturing PAGE gels were transferred to PVDF membranes. Transferring protein from native gel to PVDF membranes was conducted according to instructions for NativePAGE Novex Bis-Tris gel system. Transferred PVDF membranes were blocked with 5% milk in TBS buffer with 0.1% Tween-20 (TBST buffer) at room temperature for 1 h, and then incubated with the anti-Piezo1 antibody (1:200) at 4 °C overnight. The membranes were washed with TBST buffer and incubated with peroxidase-conjugated anti-rabbit IgG secondary antibody (1:10,000) at room temperature for 1 h. Proteins were detected with the ECL plus detection kit (GE Healthcare).

Mass spectrometry. Purified samples were separated on the 3–12% NativePAGE Novex Bis-Tris gel and visualized by fast Coomassie G-250 staining. The gel band containing the MmPiezo1–GST complex or the corresponding blank band from the control sample near the 1,236 kDa molecular marker was excised and subjected to the Scripps Center for Mass Spectrometry for analysis. In brief, the gel bands were destained, reduced with 10 mM DTT, alkylated with 55 mM iodoacetamide, and digested with Trypsin overnight before analysis using the nano-LC-MS/MS. The nano-LC-MS/MS data obtained on a LTQ ion trap mass spectrometer was searched using the MmPiezo1–GST protein sequence and NCBInr *Homo sapiens* database. In separate sets of experiments, the purified MmPiezo1–GST and control solution samples before gel electrophoresis were subjected to mass spectrometry (Supplementary Table 2).

Reconstitution into proteoliposomes or DIBs, single channel recordings and analysis. Purified MmPiezo1–GST protein was reconstituted into asolectin (soybean polar lipid extract, Avanti) liposomes (10 mg ml^{-1}) by incubating the mixture (lipid/protein mass ratios between 2,000:1 and 1,000:1; this corresponds to a molar lipid/protein ratio of ~800,000–400,000:1) on ice for 5 min followed by ×20 dilution in 200 mM KCl, 5 mM MOPS pH 7.0 and incubated with rotation at room temperature for 20 min. Biobeads were added to mixture and incubated with rotation for 1 h. Thereafter, biobeads were removed by filtration and a new batch of beads was added. After 30 min incubation, the biobeads were filtered and the sample was centrifuged at 60,000 r.p.m. for 60 min at 8 °C. The proteoliposome pellet was re-suspended in 40 µl of the same buffer and used to place two 25 µl drops on a cover slide. The samples were dried under vacuum for >16 h at 4 °C. Samples were hydrated with 25 µl of the same buffer and allowed to sit for 2 h before starting recordings. Thereafter, 2–3 µl of proteoliposomes were withdrawn from the edge of the spots on the cover slide and transferred to the recording chamber. After 5 min, the chamber was slowly filled with recording solution. Multi-GΩ seals were made to proteoliposomes immobilized at the bottom of the recording chamber. At that time, the proteoliposome patch was excised and brought through the air–water interface. Excised patches were used[35]. Pipette and bath solution contained (in mM) 200 KCl, 5 MOPS titrated to pH 7.0 with KOH. Capillaries of borosilicate glass from Sigma were pulled to yield resistances of 1–2 MΩ when immersed in recording solution.

Droplet interface lipid bilayers (DIBs) were formed between two lipid monolayer-encased aqueous nanolitre droplets submerged in hexadecane[23]. Liposomes were composed of 1,2-diphytanoyl-*sn*-glycero-3 phosphocholine (DPhPC) or 90% (mole/mole) DPhPC and 10% of the negatively charged lipid, 1,2-dioleoyl-*sn*-glycero-3-phosphatidic acid (DOPA) (Avanti Polar Lipids). MmPiezo1 was diluted directly into the liposome suspension to yield a final concentration of 2–5 ng ml^{-1}. The electrode carrying the droplet with MmPiezo1 and desired buffer–lipid mix (in mM, 500 KCl, 10 HEPES, pH 7.4, 0.5 lipid solution of DPhPC) was connected to the grounded end of the amplifier head-stage (Axopatch 200B). The second electrode, in a droplet containing the same buffer and 10% DOPA:90% DPhPC, was connected to the working end of the head-stage. Where indicated, ruthenium red or 0.2 M NaCl was injected using a nano-injector (WPI, Inc.).

For proteoliposome patches, records were acquired at a sampling frequency of 40 kHz and filtered online to 5 kHz with a 3-pole Bessel filter before digitization; for DIBs, data acquisition was at 10 kHz and filtered at 2 kHz. For analysis and presentation, records were filtered to 1 kHz with a low-pass Gaussian filter. Transitions were detected by the half-threshold method implemented in Clampfit (proteoliposomes) and by the segmental *k*-means method (SKM) implemented in QuB (DIBs). Transitions ≤0.5 ms were excluded from the pool for analysis to correct for detection of false and missed events. Data were analysed using Clampfit v.9.2 software (Axon Instruments), QuB, Excel 2007 (Microsoft), and IGOR Pro (Wavemetrics). γ was calculated from Gaussian fits to currents histograms. All statistical values represent mean ± s.e.m., unless otherwise indicated. *n* and *N* denote number of experiments and number of events, respectively. All experiments were done at room temperature.

34. Schagger, H., Cramer, W. A. & von Jagow, G. Analysis of molecular masses and oligomeric states of protein complexes by blue native electrophoresis and isolation of membrane protein complexes by two-dimensional native electrophoresis. *Anal. Biochem.* **217,** 220–230 (1994).
35. Gambale, F. & Montal, M. Voltage-gated sodium channels expressed in the human cerebellar medulloblastoma cell line TE671. *Brain Res. Mol. Brain Res.* **7,** 123–129 (1990).